Report 18-103, DESY, Hamburg
Fundamental characteristics of transverse deflecting fields

Valentin V. Paramonov*
Institute for Nuclear Research, 117312, Moscow, Russia

Klaus Floettmann
DESY, Notkestr. 85, 22603 Hamburg, Germany

The Panofsky-Wenzel theorem connects the transverse deflecting force in an rf structure with the existence of a longitudinal electric field component. In this paper it is shown that a transverse deflecting force is always accompanied by an additional longitudinal magnetic field component which leads to an emittance growth in the direction perpendicular to the transverse force. Transverse deflecting waves can thus not be described by pure TM or TE modes, but require a linear combination of basis modes for their representation. The mode description is preferably performed in the HM–HE basis to avoid converge problems, which are fundamental for the TM–TE basis.

PACS numbers: 29.27.-a, 41.85-p, 07.78.+s

I. INTRODUCTION

Transverse deflecting rf fields find numerous applications in modern particle accelerators for example as particle separators [1] or fast rf deflectors [2], as streaking device for diagnostics purposes [3], in emittance exchange beam lines [4] or as crab cavities in circular colliders as the LHC [5]. It is well known, that a beam passing through a transverse deflecting field will not only receive the desired phase dependent transverse momentum, but it will also change its energy spread due to a longitudinal electric field component which varies over the transverse size of the beam. The fundamental relation of the transverse gradient of the longitudinal electric field component and the transverse momentum was formulated by Panofsky and Wenzel in their seminal paper in 1956 [6]. Originally derived in the context of transverse deflecting rf structures, which is also the focus of this paper, the Panofsky-Wenzel theorem became a fundamental relation also for the discussion of wake potentials [7] and devices as pickups and kickers [8].
Complementary to the longitudinal electric field component a longitudinal magnetic field component exists in transverse deflecting rf fields which has been widely ignored so far. The existence of the longitudinal magnetic component requires to revisit the general mode description of transverse deflecting rf structures. Due to the coupling of the transverse motion to the longitudinal magnetic field it leads to a small, but fundamental contribution to the transverse beam emittance in the direction perpendicular to the transverse force.

*Electronic address: paramono@inr.ru,

II. SUPPORTING STRUCTURE

To provide an effective interaction between a particle, moving with the velocity $v_z = \beta_z c$, and an electromagnetic rf field it is necessary to match the phase velocity v_{ph} of a harmonic field component to the velocity of the particle. Since the phase velocity in a simple waveguide is higher than the speed of light c, while $\beta_z \leq 1.0$ it is necessary to slow down the wave in an appropriate structure.
Commonly periodically iris loaded structures as the example shown in Fig. 1, left, are employed to achieve this. The field distribution in a periodical structure represents a sum of spatial harmonics and by proper selection of the period length $d = \frac{\beta_z \lambda \theta}{2\pi}$, $0 \leq \theta \leq \pi$ a synchronous harmonic can be generated. θ is the phase advance per period and the wavelength λ for this kind of structures is typically in the range of 20-3 cm (L– to X–band). A fundamental property of periodical structures is the appearance of spatial harmonics which lead to nonlinearities in the field distribution. The nonlinearities can not be completely eliminated but they can be minimized in the region occupied by the beam by a proper design of the structure [9, 10].

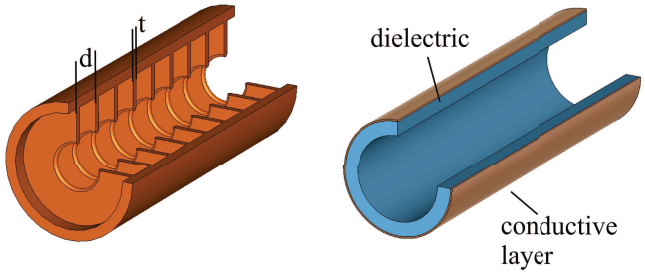

FIG. 1: Supporting structures for slow deflecting waves: periodical iris loaded circular waveguide, left, and dielectric lined waveguide, right.

Spatial harmonics do not appear in structures which are uniform in the longitudinal z direction. To slow down the wave the structure can be partially filled with a dielectric medium (see Fig. 1, right) but also thin metallic layers [11] or even a rough surface [12] can lead to slow waves.
Dielectric lined waveguides have been discussed already in the 1960s [13, 14] as candidates for beam separators operating at typical rf frequencies (3 GHz). They gain now interest again as streaking device for diagnostics purposes operating in the sub-THz to THz range [15], where the dimensions are so small that the production of periodical structures reaches technical limits. The demand to resolve ever shorter bunch length and also the progress in the generation of THz pulses of sufficient power and pulse length [16] are driving forces of these developments. Moreover, the absence of spatial harmonics makes dielectric lined waveguides also attractive from the beam dynamics point of view, because undesired side effects, like undesired emittance contributions, are minimized to their fundamental limits.

III. GENERAL RELATIONS AND MODE DESCRIPTION

The transverse deflecting force $\vec{F}_\perp$ acting on a particle moving along the longitudinal axis z with the velocity $\vec{V} = \vec{i}_z v_z$ is defined by the transverse components of the Lorentz force

$$\begin{aligned} \vec{F}_\perp &= e(E_x - v_z B_y)\vec{i}_x + e(E_y + v_z B_x)\vec{i}_y, \\ \vec{F}_\perp &= e(E_r - v_z B_\vartheta)\vec{i}_r + e(E_\vartheta + v_z B_r)\vec{i}_\vartheta, \end{aligned} \tag{1}$$

where $\vec{i}_x, \vec{i}_y, \vec{i}_z$ and $\vec{i}_\vartheta, \vec{i}_r, \vec{i}_z$ are the basis vectors of the Cartesian and cylindrical coordinate system, respectively.
The fundamental relations of deflecting field components and the corresponding longitudinal electric and magnetic field components follow directly from Maxwell's equations $\mathrm{curl}\vec{E} = -\frac{\partial}{\partial t}\vec{B}$ and $\mathrm{curl}\vec{B} = \frac{\partial}{\partial t}\frac{\vec{E}}{c^2}$ as:

$$\begin{aligned} \frac{\partial}{\partial x}E_z &= \frac{\partial}{\partial z}E_x + \frac{\partial}{\partial t}B_y, \\ \frac{\partial}{\partial y}cB_z &= \frac{\partial}{\partial t}\frac{E_x}{c} + \frac{\partial}{\partial z}cB_y. \end{aligned} \tag{2}$$

For a wave oscillating with frequency ω and wavenumber $k_z = \omega/v_{ph}$ as $\propto \mathrm{e}^{i(\omega t - k_z z)}$ the relation $\frac{1}{\partial t} = -\frac{v_{ph}}{\partial z}$ holds, thus

$$\begin{aligned} \frac{\partial}{\partial x}E_z &= \frac{\partial}{\partial z}\left(E_x - v_{ph}B_y\right), \\ -\frac{\partial}{\partial y}cB_z &= \frac{\partial}{\partial z}\left(\frac{v_{ph}}{c}E_x - cB_y\right). \end{aligned} \tag{3}$$

Equivalent transformations can be applied to the E_y and B_x components, resulting in

$$\begin{aligned} \frac{\partial}{\partial y}E_z &= \frac{\partial}{\partial z}\left(E_y + v_{ph}B_x\right), \\ \frac{\partial}{\partial x}cB_z &= \frac{\partial}{\partial z}\left(\frac{v_{ph}}{c}E_y + cB_x\right). \end{aligned} \tag{4}$$

For a particle, traveling with longitudinal velocity component $v_z = v_{ph}$ synchronously with the wave, the first equations in Eqs 3 and 4 mean:

$$\frac{1}{e}\frac{\partial}{\partial z}\vec{F}_\perp = -\frac{1}{ev_{ph}}\frac{\partial}{\partial t}\vec{F}_\perp = -i\frac{k_z}{e}\vec{F}_\perp = \vec{\nabla}_\perp E_z, \tag{5}$$

where $\vec{\nabla}_\perp = \vec{i}_x\frac{\partial}{\partial x} + \vec{i}_y\frac{\partial}{\partial y}$, see [17] and references therein.
A synchronous transverse force $\vec{F}_t \neq 0$ can thus only exist together with a longitudinal component of the electric field E_z in a deflecting rf field. The second equations in Eqs 3 and 4 necessarily require the simultaneous existence of a longitudinal magnetic field component and for the particular case $v_z = v_{ph} = c$ the relation

$$c\left[\vec{i}_z \times \vec{\nabla}B_z\right]_\perp = -i\frac{k_z}{e}\vec{F}_\perp = \vec{\nabla}_\perp E_z, \tag{6}$$

holds.
A transverse force $\vec{F}_\perp$ is thus accompanied by both, a longitudinal electric, as well as a longitudinal magnetic field component.
A general cylindrical symmetric representation of the electro-magnetic fields in vacuum in a finite domain including the symmetry axis can be based on Hertzian basis vectors, see reference [18] and references therein for a general discussion. Table I summarizes the transverse TM–TE and the hybrid HM–HE basis vectors, as introduced in [18], with a modified notation (e.g. $\vec{H}$ has been replaced by $\vec{B}$). Here $k_0 = \omega/c$, $k_z = \omega/v_{ph}$ and $k_r^2 = k_0^2 - k_z^2$ is used, while $n \in \mathbb{N}$ defines the azimuthal dependence.

The expressions of the basis vectors in Table I are presented for $v_{ph} > c$ and $k_r^2 > 0$. For waves with $v_{ph} < c$, k_r becomes imaginary and the modified Bessel functions should be used to describe the radial dependencies of the field components.
In the domain under consideration any field component G can be described by a linear combination of the basis vectors as:

$$G = A\times TM + B\times TE \quad \text{or} \quad G = P\times HM + Q\times HE \tag{7}$$

The coefficients A, B, P and Q are determined by the boundary conditions and the energy balance of the problem under consideration.
The traditional nomenclature of modes builds up on the TM–TE basis of transverse waves, which is well suited and usually applied for the field description in rf engineering and for modes with $n = 0$ symmetry, as e.g. accelerating modes. TM (Transverse Magnetic) and TE

TABLE I: TM–TE and HM–HE basis vectors $\left(J_n = J_n(rk_r),\ J'_n = \frac{\partial J_n(k_r r)}{\partial(k_r r)} = \frac{nJ_n(k_r r)}{k_r r} - J_{n+1}(k_r r)\right)$.

	TM	TE	HM	HE	azimuthal dependence	spatio-temporal dependence
E_r	$-k_z\frac{J'_n}{k_r^{n-1}}$	$-\frac{nk_0}{r}\frac{J_n}{k_r^n}$	$k_0k_z\frac{J_{n+1}}{k_r^{n+1}}$	$k_z^2\frac{J_{n+1}}{k_r^{n+1}} + \frac{n}{r}\frac{J_n}{k_r^n}$	$\cos(-n\vartheta)$	$ie^{i(\omega t-k_z z)}$
E_ϑ	$\frac{nk_z}{r}\frac{J_n}{k_r^n}$	$k_0\frac{J'_n}{k_r^{n-1}}$	$k_0k_z\frac{J_{n+1}}{k_r^{n+1}}$	$k_0^2\frac{J_{n+1}}{k_r^{n+1}} - \frac{n}{r}\frac{J_n}{k_r^n}$	$\sin(n\vartheta)$	$ie^{i(\omega t-k_z z)}$
E_z	$k_r^2\frac{J_n}{k_r^n}$	0	$k_0\frac{J_n}{k_r^n}$	$k_z\frac{J_n}{k_r^n}$	$\cos(-n\vartheta)$	$e^{i(\omega t-k_z z)}$
cB_r	$-\frac{nk_0}{r}\frac{J_n}{k_r^n}$	$-k_z\frac{J'_n}{k_r^{n-1}}$	$-k_z^2\frac{J_{n+1}}{k_r^{n+1}} - \frac{n}{r}\frac{J_n}{k_r^n}$	$-k_0k_z\frac{J_{n+1}}{k_r^{n+1}}$	$\sin(n\vartheta)$	$ie^{i(\omega t-k_z z)}$
cB_ϑ	$-k_0\frac{J'_n}{k_r^{n-1}}$	$-\frac{nk_z}{r}\frac{J_n}{k_r^n}$	$k_0^2\frac{J_{n+1}}{k_r^{n+1}} - \frac{n}{r}\frac{J_n}{k_r^n}$	$k_0k_z\frac{J_{n+1}}{k_r^{n+1}}$	$\cos(-n\vartheta)$	$ie^{i(\omega t-k_z z)}$
cB_z	0	$k_r^2\frac{J_n}{k_r^n}$	$-k_z\frac{J_n}{k_r^n}$	$-k_0\frac{J_n}{k_r^n}$	$\sin(n\vartheta)$	$e^{i(\omega t-k_z z)}$

(Transverse Electric) waves have each only one longitudinal field component; for TM waves $E_z \neq 0, B_z = 0$ and for TE waves $E_z = 0, B_z \neq 0$. It is common practice to assume that the longitudinal field components and thus the coefficients A and B are independent; the discussion above shows however that this is not the general case for $n \geq 1$.

The general solution of the boundary conditions has thus six field components and requires the linear combination of two basis vectors, either TM and TE or HM and HE. Only for $n = 0$ two separate solutions with three field components each can be formulated.

The TM-TE basis exhibits a methodical convergence problem when the phase velocity approaches c. For $v_{ph} \to c$, $k_z \to k_0$, $k_r \to 0$ the longitudinal components E_z and cB_z vanish as k_r^2. In addition all transverse field components vanish for $n = 0$ but remain finite for $n \geq 1$, cf. Table I.

Comparing the longitudinal field components by means of Eq. 7 yields the following relations of the coefficients of the two basis:

$$A = -\frac{Pk_0 + Qk_z}{k_r^2}, \quad B = \frac{Pk_z + Qk_0}{k_r^2}. \tag{8}$$

A and B are thus divergent $\propto k_r^{-2}$ when k_r approaches zero. Thus, while the basis vectors converge to zero, the product of basis vectors with the vector coefficients does not converge to zero and the field description is possible also in the limit $v_{ph} = c$.

By means of the relations Eq. 8 and the identity $J'_n = \frac{nJ_n}{rk_r} - J_{n+1}$ the complete equivalence of the two basis can be shown. The deflecting field representation for the transverse modes in a dielectric lined waveguide by Chang and Dawson [14] in the TM–TE basis is hence essentially the same as the earlier result of Vagin and Kotov [13] in the HM–HE basis.

The HM–HE basis has no convergence problem, i.e. no component of the basis converges to zero in the limit $k_r \to 0$ irrespective of n. Since each basis vector contains simultaneously electric and magnetic longitudinal vector components both, linear combinations and also pure HM or HE modes can satisfy the boundary conditions as well as Eq. 5 and 6 for $n \geq 1$.

The description of pure TM or TE modes in the HM–HE basis leads to fixed relations of the vector coefficients as $B = 0, k_z P = -k_0 Q, A = -\frac{P}{k_0}$ for TM modes and $A = 0$, $k_0 P = k_z Q$, $B = \frac{Q}{k_0}$ for TE modes. Still A or B need to be divergent in the limit $k_r \to 0$ thus also P and Q get divergent while the vector components of the hybrid basis don't converge to zero. Thus only the sum of HM and HE remains finite in this case.

The TM–TE basis is therefore preferable for the field description in the case $n = 0$, while the HM–HE basis is advantageous for $n \geq 1$.

IV. DEFLECTING FIELD FOR THE RELATIVISTIC CASE

For the relativistic case $\beta_z = 1, v_{ph} = c, k_0 = k_z, k_r = 0$ the Helmholtz wave equation reduces to the Laplace equation. In the HM–HE representation all basis vectors remain $\neq 0$ and continuous with respect to k_r. Expressions for the field components are found as limits for $k_r \to 0$ from the general form in Table I by expanding the Bessel function as:

$$\lim_{k_r \to 0} \frac{J_n(k_r r)}{k_r^n} = \frac{r^n}{2^n n!}. \tag{9}$$

The results of these transformations are summarized in Table II. Similar expressions can be found in [17], [18] and [13].

Following Table II the field distribution of the synchronous deflecting wave, $n = 1, v_{ph} = c$ in the region of the interaction with the beam is:

$$\begin{aligned}
E_z &= [P+Q]\,\frac{k_0 r}{2}\cos(\vartheta)\mathrm{e}^{i(\omega t-k_0 z)},\\
E_r &= i\left[P\frac{k_0^2r^2}{8}+Q\left(\frac{k_0^2r^2}{8}+\frac{1}{2}\right)\right]\cos(\vartheta)\mathrm{e}^{i(\omega t-k_0 z)},\\
E_\vartheta &= i\left[P\frac{k_0^2r^2}{8}+Q\left(\frac{k_0^2r^2}{8}-\frac{1}{2}\right)\right]\sin(\vartheta)\mathrm{e}^{i(\omega t-k_0 z)},\\
cB_z &= -\,[P+Q]\,\frac{k_0 r}{2}\sin(\vartheta)\mathrm{e}^{i(\omega t-k_0 z)},\\
cB_r &= -i\left[P\left(\frac{k_0^2r^2}{8}+\frac{1}{2}\right)+Q\frac{k_0^2r^2}{8}\right]\sin(\vartheta)\mathrm{e}^{i(\omega t-k_0 z)},\\
cB_\vartheta &= i\left[P\left(\frac{k_0^2r^2}{8}-\frac{1}{2}\right)+Q\frac{k_0^2r^2}{8}\right]\cos(\vartheta)\mathrm{e}^{i(\omega t-k_0 z)},
\end{aligned} \tag{10}$$

Eq. 10 describes for example the field in a dielectric lined waveguide [13].

For periodically iris loaded structures approximated expressions for the field components of the fundamental spatial harmonics inside the aperture $0 \le r \le a$ were obtained by means of the so-called small pitch approximation as (cf. [17]):

$$\begin{aligned}
E_z &= \hat{E}\frac{k_0 r}{2}\cos(\vartheta)\mathrm{e}^{i(\omega t-k_0 z)},\\
E_r &= i\hat{E}\left[\frac{k_0^2r^2+k_0^2a^2}{8}\right]\cos(\vartheta)\mathrm{e}^{i(\omega t-k_0 z)},\\
E_\vartheta &= i\hat{E}\left[\frac{k_0^2r^2-k_0^2a^2}{8}\right]\sin(\vartheta)\mathrm{e}^{i(\omega t-k_0 z)},\\
cB_z &= -\hat{E}\frac{k_0 r}{2}\sin(\vartheta)\mathrm{e}^{i(\omega t-k_0 z)},\\
cB_r &= -i\hat{E}\left[\frac{4+k_0^2r^2-k_0^2a^2}{8}\right]\sin(\vartheta)\mathrm{e}^{i(\omega t-k_0 z)},\\
cB_\vartheta &= i\hat{E}\left[\frac{4-k_0^2r^2-k_0^2a^2}{8}\right]\cos(\vartheta)\mathrm{e}^{i(\omega t-k_0 z)},
\end{aligned} \tag{11}$$

The small pitch approximation requires that $v_{ph} = c$, that the cell length d is shorter than the wavelength, $d \ll \lambda$, and that the iris thickness t is smaller than the cell length, $t \ll d$, see Fig. 1, left. Furthermore it demands that the boundary condition $E_\vartheta = 0$ is met at the aperture radius of the iris $r = a$.

A comparison of Eq. 10 and 11 yields

$$\begin{aligned}
&P+Q=\hat{E}, \quad P/Q=\frac{4}{k_0^2a^2}-1,\\
&Q=\hat{E}\frac{k_0^2a^2}{4}, \quad P=\hat{E}\left(1-\frac{k_0^2a^2}{4}\right).
\end{aligned} \tag{12}$$

The expression of the field components in Eq. 11 are thus a particular case of the more general relations in Eq. 10, i.e. the expression for the deflecting field components in Eq. 10 is valid for both, the wave in the longitudinally homogeneous dielectric lined waveguide and for the synchronous spatial harmonics in the periodically iris loaded structure.

The transverse force, Eq. 1, follows from Eq. 10 for $v_z = c$ as:

$$\begin{aligned}
F_r &= ie\frac{P+Q}{2}\cos(\vartheta)\mathrm{e}^{i(\omega t-k_0 z)} = ie\frac{\hat{E}}{2}\cos(\vartheta)\mathrm{e}^{i(\omega t-k_0 z)},\\
F_\vartheta &= -ie\frac{P+Q}{2}\sin(\vartheta)\mathrm{e}^{i(\omega t-k_0 z)} = -ie\frac{\hat{E}}{2}\sin(\vartheta)\mathrm{e}^{i(\omega t-k_0 z)},
\end{aligned} \tag{13}$$

or, transferring to Cartesian coordinates, as:

$$\begin{aligned}
F_x &= ie\frac{\hat{E}}{2}\mathrm{e}^{i(\omega t-k_0 z)},\\
F_y &= 0,\\
E_z &= \frac{\hat{E}}{2}k_0 x\mathrm{e}^{i(\omega t-k_0 z)},\\
cB_z &= -\frac{\hat{E}}{2}k_0 y\mathrm{e}^{i(\omega t-k_0 z)}.
\end{aligned} \tag{14}$$

For the synchronous relativistic case $v_{ph} = v_z = c$ the deflecting force, or equivalently the deflecting field, is in the region of of the interaction $0 \le r \le a$ constant. The longitudinal field components are shifted by $\pi/2$ in the spatio-temporal phase and rise linearly with the distance from the axis.

According to Eq. 12 is the deflecting field distributions in axially symmetric iris loaded structures for typical values of wave number k_0 and aperture radius a dominated by the HM mode, because $P/Q > 1$. The ratio P/Q depends on the design of the supporting structure and defines also other structure parameters, such as frequency, group velocity, effective shunt impedance and, in case of periodically loaded structures, the level of higher spatial harmonics. Periodical structures with complexer geometry than the simple iris loaded structure give additional freedom for optimizations and allows to reach an overall more attractive set of parameters [9].

V. INFLUENCE OF THE LONGITUDINAL FIELD COMPONENTS ON THE PARTICLE DYNAMICS

From Eq. 5 follows that the integrated transverse momentum transfered to a particle moving on a straight line (rigid beam approximation) through a region with an arbitrary electromagnetic field is related to the integrated longitudinal field by

$$p_\perp = -i\frac{e}{k_0 c}\int_0^L \nabla_\perp E_z dz. \tag{15}$$

Eq. 15 is referred to as Panofsky-Wenzel theorem. It is valid in this strict form only for synchronous motion with $v_z = v_{ph} = c$. (Asynchronous field components average to zero when the integration length is long enough.)

TABLE II: Hybrid HM–HE solutions for $v_{ph} = c$.

	HM	HE	azimuthal dependence	spatio-temporal dependence
E_r	$\frac{k_0^2 r^{n+1}}{2^{n+1}(n+1)!}$	$\frac{k_0^2 r^{n+1}}{2^{n+1}(n+1)!} + \frac{r^{n-1}}{2^n(n-1)!}$	$\cos(-n\vartheta)$	$ie^{i(\omega t - k_z z)}$
E_ϑ	$\frac{k_0^2 r^{n+1}}{2^{n+1}(n+1)!}$	$\frac{k_0^2 r^{n+1}}{2^{n+1}(n+1)!} - \frac{r^{n-1}}{2^n(n-1)!}$	$\sin(n\vartheta)$	$ie^{i(\omega t - k_z z)}$
E_z	$\frac{k_0 r^n}{2^n n!}$	$\frac{k_0 r^n}{2^n n!}$	$\cos(-n\vartheta)$	$e^{i(\omega t - k_z z)}$
cB_r	$-\frac{k_0^2 r^{n+1}}{2^{n+1}(n+1)!} - \frac{r^{n-1}}{2^n(n-1)!}$	$-\frac{k_0^2 r^{n+1}}{2^{n+1}(n+1)!}$	$\sin(n\vartheta)$	$ie^{i(\omega t - k_z z)}$
cB_ϑ	$\frac{k_0^2 r^{n+1}}{2^{n+1}(n+1)!} - \frac{r^{n-1}}{2^n(n-1)!}$	$\frac{k_0^2 r^{n+1}}{2^{n+1}(n+1)!}$	$\cos(-n\vartheta)$	$ie^{i(\omega t - k_z z)}$
cB_z	$-\frac{k_0 r^n}{2^n n!}$	$-\frac{k_0 r^n}{2^n n!}$	$\sin(n\vartheta)$	$e^{i(\omega t - k_z z)}$

The rigid beam approximation excludes ponderomotive forces, however, for a force like derived in Eq. 14 (fundamental spatial harmonics, $n = 1$, $v_{ph} = c$) ponderomotive forces are anyhow zero, because F_y is everywhere zero – not only one average – and F_x does not depend on x.
In accordance to Eq. 15 the transverse momentum $p_\perp = p_x$ and energy change of a bunch of particles passing through a deflecting structure of length L following Eq. 14 read as:

$$\begin{aligned} p_x &= \frac{eV}{c}\left(\sin(\varphi) + \cos(\varphi)\Delta\varphi\right) \\ E &= ek_0 V x\left(\cos(\varphi) - \sin(\varphi)\Delta\varphi\right), \end{aligned} \tag{16}$$

where $V = \frac{\hat{E}L}{2}$ is the integrated deflecting voltage and a first order Taylor expansion of the phase $\varphi = \omega t - k_0 z$ has been made. $\Delta\varphi$ denotes the position of a particle relative to the bunch center; $\Delta\varphi = -k_0\Delta z$.
While the first term in the momentum equation describes the average momentum gained by the bunch, the second term describes the spread due to the differences experienced by particles in the head and the tail of the bunch. In the fully deflecting mode, $\varphi = \pi/2$, the momentum spread is to first order zero, while it is maximal at $\varphi = 0$, the standard operation phase for cavity applications as diagnostics, crabbing and emittance exchange.
Due to the dependence of the longitudinal field on the transverse coordinate the induced energy spread is on all phases uncorrelated:

$$\sigma_E = \begin{cases} ek_0 V\sigma_x & \text{for} \quad \varphi = 0, \\ ek_0^2 V\sigma_x\sigma_z & \text{for} \quad \varphi = \dfrac{\pi}{2}, \end{cases} \tag{17}$$

with the transverse rms beam size in the streaking direction σ_x and the longitudinal rms bunch length σ_z. The Panofsky-Wenzel theorem, Eq. 15, as well as Eq. 16 and Eq. 17 describe the beam dynamics to first order. In second order the induced transverse momentum couples to the longitudinal magnetic field and the transverse particle position changes, which leads to an additional correlated energy spread of [4]

$$\frac{\Delta E^{cor}}{\Delta z} = \frac{\left(ek_0 V\right)^2}{cp_z}\frac{L}{6}, \tag{18}$$

where p_z denotes the longitudinal momentum of the particle.
The second order effects combine the cosine-like transverse momentum with the sine-like longitudinal field components, the Taylor expansion of the product is thus of the form $\frac{1}{2}\sin(2\varphi) + \cos(2\varphi)\Delta\varphi$ and Eq. 18 is therefore valid for $\varphi = 0$ and for $\varphi = \pi/2$.
The momentum in the streaking direction leads in combination with the longitudinal magnetic field also to a force in direction perpendicular to the streaking plane:

$$\hat{F}_y = e\frac{p_x}{\gamma m_0}B_z, \tag{19}$$

with the rest mass of the particle m_0 and the relativistic Lorentz factor γ. Thus

$$p_y = \frac{1}{c}\int \hat{F}_y\, dz = \frac{\left(ek_0 V\right)^2}{2c^2 p_z} y\Delta z. \tag{20}$$

The transverse momentum p_y is linear in the transverse position y, i.e. it is a focusing force, which depends however on the longitudinal position Δz in the bunch. It leads thus to a projected emittance contribution of

$$\varepsilon_y = \frac{\left(ek_0 V\right)^2}{2m_0 c^2 p_z}\sigma_y^2\sigma_z, \tag{21}$$

with the transverse rms beam size perpendicular to the streaking direction σ_y. Eq. 20 and 21 are again valid for

$\varphi = 0$ and for $\varphi = \pi/2$.
The emittance growth Eq. 21 in the direction perpendicular to the streaking force is a fundamental property of the deflecting field which doesn't depend on the design of the supporting structure or the operating mode of the cavity.
For present day beam and cavity parameters the emittance growth is very small, but it can not be eliminated. Additional transverse forces can still appear due the spatial harmonics especially in the end cells of rf structures and due to the backward traveling component in standing wave cavities. These forces average out in a first order approximation of the particle motion, but are relevant for second order effects [19, 20] and often dominate the beam dynamics in the plane perpendicular to the streaking direction.

VI. SUMMARY

Transverse deflecting rf structures find nowaday numerous applications in particle accelerators. Regardless of the design and operating mode of the supporting structure, a synchronous transverse force, generated by the common interaction of the transverse electric and magnetic field components, is always accompanied by both, electric as well as magnetic, longitudinal field components. The complete deflecting rf field has necessarily six field components and requires the representation by a linear combination of two basis vectors. The description in the HM–HE basis avoids convergence problems which are characteristic for the usual TM–TE basis for waves matched to the velocity of light.
Both, the longitudinal electric and the longitudinal magnetic field component lead to undesired and fundamental beam dynamics effects.
The longitudinal magnetic field, which has been ignored so far, in combination with the induced transverse momentum in the direction of the deflecting force, results in a small, but fundamental, emittance contribution in the direction perpendicular to the deflecting force.

VII. ACKNOWLEDGMENTS

The author VP is supported by RFMEFI62117X0014 program.

[1] L. Bellantoni, H. T. Edwards, M. McAshan et al., 'Design and Measurement of a Deflecting Mode Cavity for an RF Separator', in *Proceedings of the 2001 Particle Accelerator Conference, Chicago, IL,* (IEEE, New York, 2001).
[2] D. Alesini, F. Marcellini, A. Ghigo et al., 'The New RF Deflectors for the CTF3 Combiner Ring', in *Proceedings of the 2009 Particle Accelerator Conference, Vancouver, BC,*(TRIUMPF, Vancouver, 2011).
[3] D. Ratner, C. Behrens, Y. Ding et al., 'Time-resolved imaging of the microbunching instability and energy spread at the Linac Coherent Light Source', Phys. Rev. ST Accel. Beams 3, 030704, 2015.
[4] P. Emma, M. Cornacchia, 'Transverse to longitudinal emittance exchange', Phys. Rev. ST Accel. Beams 5, 084001, 2002.
[5] D. R. Brett, R. B. Appleby, R. De Maria et al., 'Accurate crab cavity modeling for the high luminosity Large Hadron Collider', Phys. Rev. ST Accel. Beams 17, 104001, 2014.
[6] W. K. H. Panofsky, W. A. Wenzel, 'Some considerations concerning the transverse deflection of charged particles in Radio-Frequency fields' Rev. Sci. Inst. **27**, 967, 1956.
[7] P. B. Wilson, 'Introduction to wake fields and wake potentials', AIP Conf. Proc. 184, Vol. 1, edited by M. Month and M. Dienes (AIP, New York, 1989), pp. 525.
[8] O. Lambertson, 'Dynamic Devices-Pickups and Kickers', in Physics of Accelerators, eds. M. Month and M. Dienes, AIP Conf. Proc. 153, 1414 (1987).
[9] K. Floettmann, V. Paramonov, 'Beam dynamics in transverse deflecting rf structures', Phys. Rev. ST Accel. Beams 17, 024001, 2014.
[10] V. V. Paramonov 'Field distribution analysis in deflecting structures' DESY 18-13, arXiv:1302.5306v1 (2013).
[11] M. Ivanyan, A. Grigoryan, A. Tsakanian et al., 'Narrowband impedance of a round metallic pipe with a low conductive thin layer', Phys. Rev. ST Accel. Beams 17, 021302, 2014.
[12] A. Novokhatsky, M. Timm, T. Weiland, 'The surface roughness wake field effect', Proceedings of the 1998 International Computational Accelerator Physics Conference, Monterey, 1998.
[13] V. A. Vagin, V. I. Kotov, 'Investigation of hybrid waves in a circular waveguide partially filled with dielectric', Journal of Technical Physics, Vol. 35, no. 7, p. 1273, 1965. Transl. in Soviet Physics - Technical Physics, Vol. 10, no. 7, p. 987, 1966.
[14] Ch. T. M. Chang, J. W. Dawson, 'Propagation of Electromagnetic Waves in a Partially Dielectric Filled Circular Waveguide', J. Appl. Phys. 41, 11, 1970.
[15] F. Lemery, K. Floettmann, T. Vinatier et al., 'A Transverse Deflection Structure with Dielectric-Lined Waveguide in the sub-THz regime', Procceedings of IPAC 2017, Copenhagen, 2017.
[16] F. Ahr et al., 'Narrowband terahertz generation with chirped-and-delayed laser pulses in periodically poled lithium niobate' Optics Letters 42, 11, 2017.
[17] Y. Garault, Etude d'une classe d'ondes electromagnetiques guideres: Les ondes EH application aux structures deflectrices pour les separateurs a obde progressive de particules relativistes. CERN 64-43, CERN, 1964
[18] H. Hahn 'Deflecting Mode in Circular Iris-Loaded Waveguides' Rev. Sci. Inst. **34**, 1094, 1963.
[19] S. Reiche, J. B. Rosenzweig, S. Anderson et al., 'Experimental confirmation of transverse focusing and adiabatic damping in a standing wave linear accelerator', Phys.

Rev. E56, 3572, (1997).
[20] A. Opanasenko, 'Applicability of the Panofsky-Wenzel theorem' Proceeding of IPAC 10, Kyoto, 2010.